Inorg. Chem. **2004**, *43*, 1762–1769

Experimental and Computational Studies of the Metal–Metal Stretching Vibration in $X_3M{\equiv}MX_3$ Compounds (X = Alkoxide, Alkyl, Amide)

Thomas M. Gilbert,*[,1] John C. Littrell,[2] Chad E. Talley,[2] Michael A. Vance,[2] Richard F. Dallinger,*[,3] and Robin D. Rogers*[,4]

Department of Chemistry and Biochemistry, Northern Illinois University, DeKalb, Illinois 60115, Department of Chemistry, Wabash College, Crawfordsville, Indiana 47933, and Department of Chemistry, The University of Alabama, Tuscaloosa, Alabama 35487

Received August 1, 2003

Raman spectra of a number of triply bonded M_2X_6 (M = Mo, W; X = alkoxide, alkyl) compounds have been obtained. Several exhibit a band assignable to the metal–metal stretching vibration $\nu_{M\equiv M}$. This band was not identified in earlier studies of the $M_2(NMe_2)_6$ compounds. We have attempted to correlate the Raman vibrational data with structural data from single-crystal X-ray diffraction studies. Diffraction studies of the M_2(O-1-4-pentyl-[2.2.2]bicyclooctyl)$_6$ species show a crowded environment around the dimetal core, but the M–M–O angles differ substantially from 90°. Thus, this angle does not solely determine the extent to which the metal–metal and ligand-based vibrational modes couple and, in turn, our ability to observe $\nu_{M\equiv M}$. Computational studies of model systems confirm the assignment of the band as being $\nu_{M\equiv M}$, although the predicted vibrational energies are consistently too high by ca. 7%. The computational results suggest that a $\nu_{M\equiv M}$ band may be present in the published spectra of the $M_2(NMe_2)_6$ pair.

We reported in 1997 the first experimental observation of $\nu_{M\equiv M}$, the metal−metal stretching frequency band, in the Raman spectra of triply-bonded $X_3M{\equiv}MX_3$ compounds (M = Mo, W; X = bulky alkoxide or alkyl).[5] At that time, we noted that, for X = an alkoxide, it appeared necessary that the alkoxide be tertiary for $\nu_{M\equiv M}$ to be definitively assigned. We reasoned, as had Cotton and Chisholm in their studies of the $M_2(NMe_2)_6$ dimers,[6,7] that, for $\nu_{M\equiv M}$ to be observable, it must not couple with ligand-based vibrations such as the M−M−O bending mode. Such coupling lessens as the M−M−O angle approaches 90°, which occurs when steric congestion around the oxygen atom is high, e.g., when the alkoxide is tertiary. This argument extended to systems where X = alkyl; for example, $\nu_{M\equiv M}$ was readily observed in the $M_2(CH_2SiMe_3)_6$ homologues, where one can equate the alkyl CH_2 group to the alkoxide O atom.

To test this theory, we prepared an array of M_2X_6 compounds, where X was a variety of tertiary alkoxides or bulky alkyl groups. Crystallographic and Raman spectroscopic studies indicate that the relationship between bond angle and our ability to observe $\nu_{M\equiv M}$ is not as straightforward as we had hoped. Computational studies reproduce the structures of examples of each class of triply-bonded molecules accurately when one employs augmented basis sets, but the calculated frequencies of $\nu_{M\equiv M}$ are consistently high. However, the computations confirm the assignments of $\nu_{M\equiv M}$ and allow us to suggest that bands corresponding to $\nu_{M\equiv M}$ for $M_2(NMe_2)_6$ appear in the spectra Cotton and Chisholm published. We report these studies below.

Experimental Section

$Mo_2[OC(CH_3)_3]_6$,[8] $W_2[OC(CH_3)_3]_6$,[9] Mo_2(pinacolate)$_3$,[10] W_2(pinacolate)$_3$,[11] $Mo_2[OC(CH_3)_2(CF_3)]_6$,[8] $W_2[OC(CH_3)_2(CF_3)]_6$,[8,12] Mo_2(O-

* Corresponding author.
(1) Direct correspondence regarding the syntheses and computations to this author at Northern Illinois University. E-mail: tgilbert@marilyn.chem.niu.edu.
(2) Wabash College.
(3) Direct correspondence regarding the spectroscopic experiments to this author at Wabash College. E-mail: dallingr@wabash.edu.
(4) Direct correspondence regarding the diffraction studies to this author at The University of Alabama. E-mail: RDRogers@bama.ua.edu.
(5) Littrell, J. C.; Talley, C. E.; Dallinger, R. F.; Gilbert, T. M. *Inorg. Chem.* **1997**, *36*, 760−761.
(6) Chisholm, M. H.; Cotton, F. A.; Frenz, B. A.; Reichert, W. W.; Shive, L. W.; Stults, B. R. *J. Am. Chem. Soc*. **1976**, *98*, 4469−4476.
(7) Chisholm, M. H.; Cotton, F. A.; Extine, M.; Stults, B. R. *J. Am. Chem. Soc.* **1976**, *98*, 4477−4485.
(8) Gilbert, T. M.; Landes, A. M.; Rogers, R. D. *Inorg. Chem.* **1992**, *31*, 3438−3444.
(9) Chisholm, M. H.; Eichhorn, B. W.; Folting, K.; Huffman, J. C.; Ontiveros, C. D.; Streib, W. E.; van der Sluys, W. G. *Inorg. Chem.* **1987**, *26*, 3182−3186.
(10) Gilbert, T. M.; Bauer, C. B.; Bond, A. M.; Rogers, R. D. *Polyhedron* **1999**, *18*, 1293−1301.

10.1021/ic030246f CCC: $27.50
Published on Web 02/03/2004

2,6-$C_6Me_2H_3$)$_6$,[13] W_2(O-2,6-$C_6Me_2H_3$)$_6$,[14] $Mo_2(CH_2C_6H_5)_6$,[15] $W_2(CH_2C_6H_5)_6$,[16] $Mo_2[CH_2C(CH_3)_3]_6$,[8] $W_2[CH_2C(CH_3)_3]_6$,[9] $Mo_2[CH_2Si(CH_3)_3]_6$,[8] $W_2[CH_2Si(CH_3)_3]_6$,[9,17] $Mo_2[CH_2C(CH_3)_2(C_6H_5)]_6$,[16] $Mo_2(NMe_2)_6$,[6] $W_2(NMe_2)_6$,[7] and $NaW_2Cl_7(THF)_5$[9] were prepared as described in the literature. $Mo_2[OC(CD_3)_3]_6$, $W_2[OC(CD_3)_3]_6$ Mo_2(pinacolate-d_{12})$_3$, and W_2(pinacolate-d_{12})$_3$ were prepared similarly to the proteated analogues. $LiCH_2C(CH_3)_2(C_6H_5)$ was prepared from $ClCH_2C(CH_3)_2(C_6H_5)$ and Li in refluxing pentane analogously to the synthesis of $LiCH_2CMe_3$.[18] 4-Pentyl[2.2.2]bicyclooctan-1-ol was obtained from Aldrich and was recrystallized before use.

Mo_2(O-1-adamantyl)$_6$. $Mo_2(NMe_2)_6$ (0.913 g, 2.00 mmol) was dissolved in 50 mL of toluene, and the solution was cooled to −40 °C. 1-Adamantanol (1.98 g, 13.0 mmol) was added as the solution was stirred and warmed to room temperature. After 18 h, a copious amount of red precipitate was present. The mixture was heated to 70 °C for 6 h and then cooled to room temperature. The red solid was filtered off, washed with toluene and pentane, and dried, giving 1.56 g (1.42 mmol, 71%) of orange powder. This material proved insoluble in all solvents with which it did not react. Anal. Calcd for $C_{60}H_{90}Mo_2O_6$: C, 65.56; H, 8.25; N, 0.0. Found: C, 65.63; H, 8.52; N, 0.0.

W_2(O-1-adamantyl)$_6$ was prepared similarly from $W_2(NMe_2)_6$ (1.26 g, 2.00 mmol), giving 1.90 g (1.49 mmol, 75%) of orange powder. This material proved insoluble in all solvents with which it did not react. Anal. Calcd for $C_{60}H_{90}W_2O_6$: C, 56.52; H, 7.11; N, 0.0. Found: C, 56.31; H, 7.05; N, 0.0.

Mo_2(O-1-4-pentyl[2.2.2]bicyclooctyl)$_6$. $Mo_2(NMe_2)_6$ (0.456 g, 1.00 mmol) was dissolved in 70 mL 1:1 benzene/heptane and treated with 4-pentyl[2.2.2]bicyclooctan-1-ol (1.18 g, 6.00 mmol) as the solution was stirred. After 18 h, the mixture was heated to 100 °C for 24 h and then cooled to room temperature. The solvent was evaporated in vacuo, and the resulting yellow-brown solid was triturated with $(Me_3Si)_2O$. The yellow powder was filtered out, washed with $(Me_3Si)_2O$, and dried, giving 0.71 g of product. Cooling the mother liquor to −40 °C overnight provided a second crop of material. The total yield was 0.90 g (0.66 mmol, 66%). ^{1}H NMR (C_6D_6; δ): 2.21, 1.64 (br m, 12H, ring Hs); 1.13 (br m, 8H, pentyl CH_2s); 0.89 (t, J_{HH} = 7.0 Hz, 3H, CH_3). Anal. Calcd for $C_{78}H_{138}Mo_2O_6$: C, 68.69; H, 10.20; N, 0.0. Found: C, 68.55; H, 10.64; N, 0.0.

W_2(O-1-4-pentyl[2.2.2]bicyclooctyl)$_6$ was prepared similarly from $W_2(NMe_2)_6$ (0.750 g, 1.19 mmol), giving 1.52 g (0.987 mmol, 83%) of orange powder. ^{1}H NMR (C_6D_6; δ): 2.27, 1.65 (br m, 12H, ring Hs); 1.12 (br m, 8H, pentyl CH_2s); 0.89 (t, J_{HH} = 6.7 Hz, 3H, CH_3). Anal. Calcd for $C_{78}H_{138}W_2O_6$: C, 60.85; H, 9.03; N, 0.0. Found: C, 60.84; H, 9.26; N, 0.0.

$W_2[CH_2C(CH_3)_2(C_6H_5)]_6$. A 1:1 diethyl ether/pentane solution (100 mL) of $LiCH_2C(CH_3)_2(C_6H_5)$ (1.70 g, 12.1 mmol) was cooled to −78 °C and treated with small portions of a slurry of $NaW_2Cl_7(THF)_5$ (2.00 g, 2.00 mmol) in THF (50 mL) over 15 min. The resulting green slurry was stirred 1 h at this temperature and then allowed to warm slowly to room temperature. After 18 h of stirring, the volatiles were evaporated, giving a dark semisolid. This was extracted with 4 × 25 mL portions of toluene. The extracts were filtered through Celite, giving a clear, dark red solution. The toluene was evaporated, giving a dark oil. This was dissolved in 40 mL of pentane. The pentane extracts were filtered through Celite and cooled to −40 °C. The dark red microcrystals which precipitated were filtered out, washed with CH_3CN, and dried, giving 70 mg (0.060 mmol, 3%) of product. As this was sufficient material for the Raman experiment, we did not try to optimize the yield. ^{1}H NMR (C_6D_6; δ): 7.29−7.09 (m, 5H, phenyl Hs); 2.09 (s, 2H, CH_2); 1.39 (s, 6H, CH_3).

$Mo_2[CH_2C_6H_4$-4-Me$]_6$. A slurry of $Mo_2(OCy)_6$ (590 mg, 0.750 mmol) was cooled to −30 °C and treated dropwise over 45 m with an ethereal solution of Li[$CH_2C_6H_4$-4-Me] (0.056 M, 89.0 mL, 5.00 mmol). The solution reddened immediately; toward the end of the addition, orange solid precipitated. The slurry was stirred for 30 m and then allowed to warm slowly to room temperature. The solvent was evaporated in vacuo without warming, giving orange-red powder. This was triturated with heptane and filtered out and then washed with 3 × 10 mL of heptane, 2 × 10 mL of toluene, and 1 × 10 mL of ether. The resulting orange powder was dried in vacuo, giving material sufficiently pure by ^{1}H NMR for acquisition of its Raman spectrum (535 mg, 0.650 mmol, 87%). ^{1}H NMR (C_6D_6; δ): 6.87 (d, 2H, phenyl Hs); 6.43 (d, 2H, phenyl Hs); 3.82 (s, 2H, CH_2); 2.15 (s, 3H, CH_3).

Table 1. Summary of Crystal, Data Collection, and Structure Refinement Data for M_2(O-1-4-pentyl[2.2.2]bicyclooctyl)$_6$ (M = Mo, W)

	Mo	W
T, K	296	123
cell consts (Å, deg)		
a	13.0158(4)[a]	15.242(6)[b]
b	10.8872(3)	14.724(7)
c	27.6489(8)	16.517(4)
β	100.698(1)	95.10(3)
V, Å^3	3849.9(2)	3692(1)
space group	$P2_1/c$	$P2_1/n$
Z	2	2
μ_{calc}, cm^{-1}	3.73	33.5
rel transm factors	0.99−0.84	0.99−0.46
reflcns meas'd/indpdt/obsd	14 112/5538/4641[c]	6834/6825/4832[d]
2θ range, deg	$3 \le 2\theta \le 47.2$	$3 \le 2\theta \le 49$
params	474	397
R/R_w/GOF	0.0470[e]/0.0601 (wR2)/1.044[f]	0.051[g]/0.056/1.29[h]

[a] Cell parameters were determined by least-squares refinement of ((sin θ)/λ)^2 for 2500 reflections over the full θ range. [a] Cell parameters were determined by least-squares refinement of ((sin θ)/λ)^2 for 25 reflections, $\theta \ge 20°$. [c] Considered observed if $I > 2\sigma(I)$. [d] Considered observed if $F \ge 5\sigma(F)$. [e] $R = \Sigma||F_o| - |F_c||/\Sigma|F_o|$; wR2 = $\{\Sigma w(F_o^2 - F_c^2)^2/\Sigma w(F_o^2)^2\}^{1/2}$. [f] GOF = $[\Sigma w(F_o^2 - F_c^2)^2/(N_o - N_v)]^{1/2}$; N_o = number of observations, N_v = number of variables. [g] $R = \Sigma||F_o| - |F_c||/\Sigma|F_o|$; $R_w = \{\Sigma w(|F_o| - |F_c|)^2/\Sigma w(F_o)^2\}^{1/2}$. [h] GOF = $[\Sigma w(|F_o| - |F_c|)^2/(N_o - N_v)]^{1/2}$; N_o = number of observations, N_v = number of variables.

Single-Crystal X-ray Diffraction Studies of M_2(O-1-4-pentyl-[2.2.2]bicyclooctyl)$_6$ (M = Mo, W). Single crystals of both compounds were grown by slow diffusion of pentane into concentrated toluene solutions of the materials at −40 °C. Handling procedures have appeared elsewhere.[10] Data were collected using Mo Kα radiation (λ = 0.710 73 Å) on either a Siemens SMART diffractometer equipped with a CCD area detector (M = Mo) or an Enraf-Nonius CAD-4 using $\omega-2\theta$ scans (M = W). Data collection and refinement parameters appear in Table 1. The data were corrected for Lorentz/polarization effects, empirically corrected

(11) Chisholm, M. H.; Folting, K.; Hampden-Smith, M.; Smith, C. A. *Polyhedron* **1987**, *6*, 1747−1755.
(12) Freudenberger, J. H.; Pedersen, S. F.; Schrock, R. R. *Bull. Soc. Chim. Fr.* **1985**, 349−352.
(13) Coffindaffer, T. W.; Rothwell, I. P.; Huffman, J. C. *Inorg. Chem.* **1983**, *22*, 2906−2910.
(14) Latham, I. A.; Sita, L. R.; Schrock, R. R. *Organometallics* **1986**, *5*, 1508−1510.
(15) Beshouri, S. M.; Rothwell, I. P.; Folting, K.; Huffman, J. C.; Streib, W. E. *Polyhedron* **1986**, *5*, 1191−1195.
(16) Gilbert, T. M.; Bauer, C. B.; Rogers, R. D. *Polyhedron* **1999**, *18*, 1303−1310.
(17) Chisholm, M. H.; Cotton, F. A.; Extine, M.; Stults, B. R. *Inorg. Chem.* **1976**, *15*, 2252−2257.
(18) Schrock, R. R.; Fellmann, J. D. *J. Am. Chem. Soc.* **1978**, *100*, 3359−3370.

Table 2. Selected Bond Lengths (Å) and Angles (deg) for M_2(O-1-4-pentyl[2.2.2]bicyclooctyl)$_6$ (M = Mo, W)

Mo		W	
Mo≡Mo[a]	2.2581(7)	W≡W[b]	2.3407(6)
Mo'≡Mo' [a,c]	2.225(6)		
Mo−O(1)	1.889(2)	W−O(1)	1.910(5)
Mo−O(2)	1.873(3)	W−O(2)	1.867(5)
Mo−O(3)	1.900(2)	W−O(3)	1.867(5)
O(1)−C(1)	1.430(4)	O(1)−C(1)	1.459(9)
O(2)−C(14)	1.448(4)	O(2)−C(14)	1.438(9)
O(3)−C(27)	1.449(4)	O(3)−C(27)	1.448(9)
O(2)−Mo−O(1)	110.91(12)	O(1)−W−O(2)	111.7(2)
O(2)−Mo−O(3)	115.90(12)	O(1)−W−O(3)	118.4(2)
O(1)−Mo−O(3)	114.27(11)	O(2)−W−O(3)	106.5(2)
Mo−Mo−O(1)	107.45(8)	W−W−O(1)	100.0(2)
Mo−Mo−O(2)	107.86(9)	W−W−O(2)	110.5(2)
Mo−Mo−O(3)	99.28(7)	W−W−O(3)	109.5(2)
Mo−O(1)−C(1)	142.8(2)	W−O(1)−C(1)	123.0(5)
Mo−O(2)−C(14)	154.1(2)	W−O(2)−C(14)	149.4(5)
Mo−O(3)−C(27)	122.2(2)	W−O(3)−C(27)	146.5(5)

[a] Symmetry code = $-x+1, -y, -z+1$. [b] Symmetry code = $-x, 2-y, -z$. [c] Atom refined at 10% occupancy; remainder of contacts not listed.

for absorption using either ψ-scans (M = W) or simulated ψ-scans from area detector data (M = Mo), and refined using either SHELXS[19] and SHELX[20] or SHELXTL.[21] All non-hydrogen atoms were refined with anisotropic thermal parameters. Hydrogen atoms were placed in calculated positions 0.95 Å from the bonded carbon atom and allowed to ride on that carbon, with isotropic thermal parameters $U(\mathrm{H}) = 1.2U_{\mathrm{eqv}}(\mathrm{C})$ (M = Mo) or $B(\mathrm{H}) = 5.5$ Å^2 (M = W).

Important bond lengths and angle are given in Table 2. A Molecule[22] drawing based on the crystallographic coordinates of the major contributor of the molybdenum dimer (see below) appears in Figure 1. The tungsten dimer is structurally similar.

The dimolybdenum compound exhibited two types of disorder. First, one ligand was rotationally disordered. Two orientations were resolved for the three ethylene bridges of the bicyclooctyl moiety. The atoms C28, C29, C31, C32, C33, and C34 and their disorder correspondents refined at 50% occupancy. Atoms C27, C30, C35, C36, and C37 were included at 100% occupancy, although the thermal motion for C35−C37 (in the five-carbon chain) is high. Disorder in the chain could only be resolved for the terminal methyl group and the preceding methylene group. C38 and C39 were resolved into two positions and refined at 50% occupancy each. The thermal parameters and esds for this entire ligand are larger than those for the two ordered ligands, reflecting its disordered nature.

The second type of disorder involves the Mo position and is often seen in M_2X_6 structures. A large peak representing 10% of the Mo positions was observed ca. 1.1 Å from the main Mo position. The Mo−Mo core occupies two orientations, while the six O ligands occupy only one. Thus, Mo is coordinated to O1, O2, and O3, while Mo′ is coordinated to O1, O3, and O2a (the last related by a center of inversion). The Mo position describes 90% of the Mo−Mo units, and the Mo−O bond lengths corresponding to this position are normal. The Mo′ position represents only 10% of the Mo′−Mo′ units, and the Mo′−O distances are distorted. This most likely arises from the fact that the experiment cannot resolve small (10%) variations in the O positions.

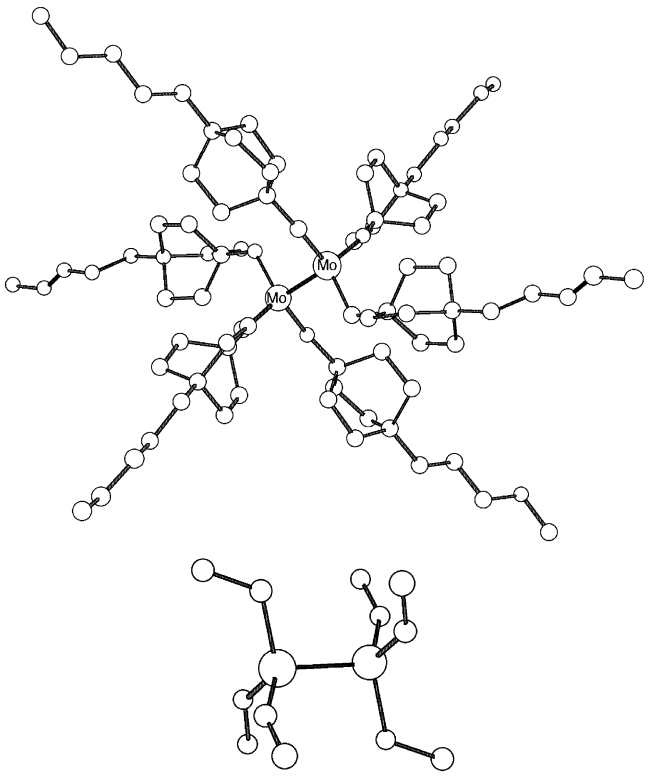

Figure 1. Molecule[22] diagram of the major contributor to the structure of Mo_2(O-1-4-pentyl[2.2.2]bicyclooctyl)$_6$. Hydrogen atoms were removed for clarity. The inset shows the molecular core and the "two proximal, one distal" configuration of the alkoxide ligands.

Raman Spectroscopy. Raman spectra of solids in sealed melting point capillaries were obtained using 632.8-nm excitation from a He−Ne laser (Uniphase model 1135P). Nonlasing emission lines from the laser were eliminated with a band-pass filter (Melles Griot, 632.8 nm, 3 nm fwhm). The laser power at the sample was measured to be 7 mW. Backscattered Raman radiation was dispersed with a 0.85-m SPEX model 1403 double monochromator with a spectral slit width of 4.0 cm^{-1}. The Raman signal was detected by a cooled Hamamatsu R928 photomultiplier tube and processed by a Stanford Research Systems model SR4000 photon-counting system. The spectrometer was calibrated daily with the Raman bands of CCl_4, and we believe our peak frequencies to be good to ±2 cm^{-1}.

Computational Structure Optimizations and Frequency Calculations. Optimizations and analytical frequency calculations were performed using the Gaussian 98 (G98) suite of programs,[23] using the B3LYP model chemistry[24] and the basis sets[25] given in Table

(19) Sheldrick, G. M. *Acta Crystallogr., Sect. A* **1990**, *46*, 467−473.
(20) Sheldrick, G. M. *SHELX76, a suite of computer programs for X-ray structure determination, as locally modified*; University of Cambridge: Cambridge, England, 1976.
(21) Sheldrick, G. *SHELXTL, a suite of computer programs for X-ray structure determination*; Siemens Analytical Instruments, Inc.: Madison, WI, 1997.
(22) van Eikema Hommes, N. J. R. *Molecule for Macintosh*, version 1.3.5d9; 1999.
(23) Frisch, M. J.; Trucks, G. W.; Schlegel, H. B.; Scuseria, G. E.; Robb, M. A.; Cheeseman, J. R.; Zakrzewski, V. G.; Montgomery, J. A., Jr.; Stratmann, R. E.; Burant, J. C.; Dapprich, S.; Millam, J. M.; Daniels, A. D.; Kudin, K. N.; Strain, M. C.; Farkas, O.; Tomasi, J.; Barone, V.; Cossi, M.; Cammi, R.; Mennucci, B.; Pomelli, C.; Adamo, C.; Clifford, S.; Ochterski, J.; Petersson, G. A.; Ayala, P. Y.; Cui, Q.; Morokuma, K.; Malick, A D.; Rabuck, K. D.; Raghavachari, K.; Foresman, J. B.; Cioslowski, J.; Ortiz, J. V.; Baboul, A. G.; Stefanov, B. B.; Liu, G.; Liashenko, A.; Piskorz, P.; Komaromi, I.; Gomperts, R.; Martin, R. L.; Fox, D. J.; Keith, T.; Al-Laham, M. A.; Peng, C. Y.; Nanayakkara, A.; Challacombe, M.; Gill, P. M. W.; Johnson, B.; Chen, W.; Wong, M. W.; Andres, J. L.; Gonzalez, C.; Head-Gordon, M.; Replogle, E. S.; Pople. J. A. *Gaussian 98*, revision A.7; Gaussian, Inc.: Pittsburgh, PA, 1998.

Table 3. Experimental MM Vibrational Frequencies (cm^{-1}) for Homologous M_2X_6 Compounds (M = Mo, W)

	$\nu_{Mo{\equiv}Mo}$	$\nu_{W{\equiv}W}$	$\nu_{Mo{\equiv}Mo}/\nu_{W{\equiv}W}$
Hexaalkoxides			
$M_2[OC(CH_3)_3]_6$	386	303	1.27
$M_2[OC(CD_3)_3]_6$	363	285	1.27
M_2(O-1-adamantoxy)$_6$	369	274	1.35
M_2(pinacolate)$_3$	372	290	1.28
M_2(pinacolate-d_{12})$_3$	359	281	1.28
$M_2[OC(CH_3)_2(CF_3)]_6$	360	280	1.29
M_2(O-1-4-pentyl[2.2.2]bicyclooctyl)$_6$	379	283	1.34
M_2(O-2,6-$C_6Me_2H_3$)$_6$	356	283	1.26
av	369 ± 9^a	283 ± 7	1.29 ± 0.03
Hexaalkyls			
$M_2(CH_2C_6H_5)_6$	355	285	1.25
$M_2[CH_2C(CH_3)_3]_6$	361	292	1.24
$M_2[CH_2Si(CH_3)_3]_6$	369	299	1.23
$M_2[CH_2C(CH_3)_2(C_6H_5)]_6$	359	283	1.27
av	361 ± 9	290 ± 12	1.25 ± 0.03
overall av	366 ± 6	287 ± 5	1.28 ± 0.02

[a] Deviations are given at the 95% confidence level.

4. The LANL2DZ basis set as provided in the G98 program models first-row atoms (H, C, N, and O) using the D95V basis set and contains relativistic effective core potentials (ECPs) to simplify calculations on heavier atoms. Valence electrons on the latter are modeled using a (5s5p3d) set of functions contracted to [3s3p2d] functions. Since Hay[26] has expressed concern over whether the contraction scheme developed for Hartree−Fock approaches applies to correlation-containing models such as B3LYP, further calculations employed the uncontracted functions. These are represented in the table as LANL2DZunc. This approach was applied solely to the metal atoms. The set denoted LANL2DZunc+f is the uncontracted LANL2DZ basis set augmented with an f polarization function on each metal. When these basis sets were used to describe the metal atoms, light atoms were modeled using the standard 6-31G(d) basis set. The exponents for the f polarization functions (0.46 for Mo and 0.40 for W) were determined by minimizing the energy of the optimized structures of M_2H_6 vs the exponents, using the Gaussian utility program Gauopt. These values are similar to those derived by Martin and Sundermann for basis sets using the SDB ECPs (0.640 and 0.338, respectively).[27] They differ drastically from those suggested by Frenking et al. for augmenting a contracted LANL2DZ basis set (1.043 for Mo, 0.823 for W).[28] Because in principle Frenking's values should be more generally applicable (since they were determined for the atoms in the appropriate spin states using the CISD model), we examined the effect of using these values for the polarization function on the hexaamides $M_2(NMe_2)_6$. In both cases this gave optimized structures similar to ours, with slightly (ca. 0.008 Å) longer M≡M distances, with slightly (0.005 Å) shorter M−N distances, and of higher energy (ca. 3−6 kcal mol^{-1}). The predicted value of $\nu_{M{\equiv}M}$ for the ditungsten compound did not change; that for the dimolybdenum compound decreased slightly, from 438 to 428 cm^{-1}.

Optimizations were run without constraints, although the starting structures were based on crystallographic ones. We did not scan the torsional space to prove that the optimized structures were global minima. The frequency runs demonstrated that all optimized structures were at worst local minima and not saddle points. Optimized structural parameters and metal−metal vibrational frequencies identified in the frequency output for all molecules studied at all levels appear in Table 4. Cartesian coordinates for the six compounds studied at the B3LYP/LANL2DZunc+f;6-31G(d) level are available as Supporting Information.

Table 4. Experimental and Calculated (B3LYP Model) Structural Parameters and Frequencies for M_2X_6 Compounds[a]

	basis set[b]	M≡M	M−O	O−C	M−M−O	M−O−C	$\nu_{M{\equiv}M}$
Mo_2(O-1-4-pentyl[2.2.2]bicyclooctyl)$_6$	expt	2.2581	1.889, 1.873, 1.900	1.442	107.86, 107.45, 99.28	154.1, 142.8, 122.2	379
$Mo_2[OC(CH_3)_3]_6$	expt						386
$Mo_2[OC(CH_3)_3]_6$	DZ	2.288	1.901, 1.901, 1951	1.476	108.8, 108.4, 99.1	154.7, 154.3, 126.8	405
$Mo_2[OC(CH_3)_3]_6$	DZunc	2.291	1.902, 1.901, 1.945	1.439	109.7, 109.2, 99.4	153.3, 153.2, 125.5	401
$Mo_2[OC(CH_3)_3]_6$	DZunc+f	2.249	1.890, 1.890, 1.935	1.438	109.4, 109.0, 99.5	155.1, 154.5, 126.4	408
W_2(O-1-4-pentyl[2.2.2]bicyclooctyl)$_6$	expt	2.3407	1.867, 1.867, 1.910	1.448	110.5, 109.5, 100.0	149.4, 146.5, 123.0	283
$W_2[OC(CH_3)_3]_6$	expt						303
$W_2[OC(CH_3)_3]_6$	DZ	2.353	1.889, 1.891, 1.950	1.481	109.5, 109.3, 99.8	154.3, 154.2, 127.5	317
$W_2[OC(CH_3)_3]_6$	DZunc	2.360	1.889, 1.890, 1.941	1.443	110.3, 110.1, 100.2	152.8, 152.8, 126.4	316
$W_2[OC(CH_3)_3]_6$	DZunc+f	2.340	1.880, 1.879, 1.932	1.441	110.1, 109.9, 100.3	154.2, 154.1, 127.1	316
$Mo_2[CH_2C(CH_3)_2Ph]_6$	expt[c]	2.1765	2.138, 2.138, 2.125	1.549	97.8, 97.6, 97.8	124.9, 125.1, 126.8	359
$Mo_2[CH_2C(CH_3)_3]_6$	expt						361
$Mo_2[CH_2C(CH_3)_3]_6$	DZ	2.217	2.166	1.563	98.0	124.1	396/407
$Mo_2[CH_2C(CH_3)_3]_6$	DZunc	2.211	2.168	1.552	97.8	124.7	393
$Mo_2[CH_2C(CH_3)_3]_6$	DZunc+f	2.168	2.167	1.553	98.0	125.2	397/407/413
$W_2[CH_2Si(CH_3)_2Ph]_6$	expt[c]	2.2587	2.101, 2.116, 2.105		101.9, 102.2, 102.2		283[d]
$W_2[CH_2C(CH_3)_3]_6$	expt						292
$W_2[CH_2C(CH_3)_3]_6$	DZ	2.278	2.156	1.567	98.6	124.7	318/314
$W_2[CH_2C(CH_3)_3]_6$	DZunc	2.276	2.159	1.557	98.5	125.7	314
$W_2[CH_2C(CH_3)_3]_6$	DZunc+f	2.251	2.156	1.558	98.6	126.0	313
$Mo_2[N(CH_3)_2]_6$	expt	2.214	1.98	1.47	103.7	133.4, 116.3	
$Mo_2[N(CH_3)_2]_6$	DZ	2.247	1.996	1.480	104.3	132.0, 117.7	446
$Mo_2[N(CH_3)_2]_6$	DZunc	2.246	1.999	1.457	104.2	132.3, 117.5	437
$Mo_2[N(CH_3)_2]_6$	DZunc+f	2.209	1.992	1.457	104.2	132.6, 117.5	438
$W_2[N(CH_3)_2]_6$	expt	2.292	1.97	1.48	103.3	134, 116	
$W_2[N(CH_3)_2]_6$	DZ	2.319	1.986	1.480	104.3	132.4, 117.8	382
$W_2[N(CH_3)_2]_6$	DZunc	2.321	1.988	1.460	104.3	132.7, 117.6	376
$W_2[N(CH_3)_2]_6$	DZunc+f	2.301	1.982	1.460	104.2	132.9, 117.5	373

[a] Values are the averages of all like parameters. Distances are in Å, angles in deg, and frequencies in cm^{-1}. [b] Basis sets: DZ = LANL2DZ; DZunc = LANL2DZ uncontracted on the metal atoms, 6-31G(d) on all other atoms; DZunc+f = LANL2DZ uncontracted plus an f polarization function on the metal atoms, 6-31G(d) on all other atoms. [c] Reference 16. [d] This is actually the value of $\nu_{W{\equiv}W}$ for $W_2[CH_2C(CH_3)_2Ph]_6$, which was unambiguously observed in the Raman spectrum. Unfortunately, we have been unable to grow single crystals of this compound. No band in the spectrum of $W_2[CH_2Si(CH_3)_2Ph]_6$ could be unambiguously assigned to $\nu_{W{\equiv}W}$; however, a band tentatively assigned to this vibration appeared at 293 cm^{-1}.

Results and Discussion

Structures of M_2(O-1-4-pentyl[2.2.2]bicyclooctyl)$_6$. We prepared and examined many compounds to find those that exhibited a Raman band assignable to $\nu_{M\equiv M}$. Approximately half did so (see below), but unfortunately, most did not give crystals suitable for X-ray diffraction experiments. The M_2(pinacolate)$_3$[10,11] compounds met both criteria, but their bidentate ligand attachment to the metal core compromised study of the relationship between observation of $\nu_{M\equiv M}$ and the various molecular degrees of freedom. The hexaalkyls $M_2(CH_2SiMe_3)_6$ and $M_2(CH_2Ph)_6$ also met both criteria, but examples of hexakis(terminal tertiary alkoxide) dimers that did remained nonexistent.

Fortunately, the dimers M_2(O-1-4-pentyl[2.2.2]bicyclooctyl)$_6$ (hereafter the ligand is denoted O-bicyc*) displayed a $\nu_{M\equiv M}$ Raman band and crystallized with minimal disorder (M = Mo) or no disorder (M = W). Figure 1 shows the dimolybdenum complex (the ditungsten complex is structurally similar); Table 2 contains relevant structural data. The bond distances generally fall into the expected ranges, although the Mo≡Mo bond length of 2.252(2) Å is the longest ever reported for a homoleptic $Mo_2(OR)_6$ compound. Both molecules crystallize with one distal and two proximal alkoxides and fit the "distal/proximal" bond lengths and angles pattern established for these triply bonded systems:[10] proximal alkoxides display smaller M−O bonds and larger M−M−O and M−O−C angles, while distal alkoxides display the reverse. Of some note is that, in contrast to systems studied previously, some of the proximal ligand M−M−O−C torsion angles differ sizably from 0°. For example, while one of the torsions in the Mo_2 compound is essentially 0°, the other is 50.4°, the largest value ever observed for a proximal torsion by a wide margin. In the W_2 compound, the proximal torsions are 16 and 21°, larger than all but the one above and those in $Mo_2(OCH_2CMe_3)_4$(acac) (26°). These distortions highlight the substantial steric crowding in an M_2(terminal tertiary alkoxide)$_6$ molecule; if such a molecule crystallizes such that two proximal ligands exist, their mutual interference dictates that at least one cannot maintain "perfect proximality".

As noted above, we believed early in this work that $M_2(OR)_6$ dimers that would display a Raman band assignable to $\nu_{M\equiv M}$ would contain M−M−O angles near 90°, so as to minimize coupling between this mode and ligand-based modes. Support for this view appears in Table 4: the $M_2(CH_2R)_6$ molecules for which we observe $\nu_{M\equiv M}$ exhibit M−M−C angles ≤ 102.2°. The $M_2[N(CH_3)_2]_6$ species, for which $\nu_{M\equiv M}$ was not identified, exhibit M−M−N angles ≥ 103.3°.[6,7] The difference between these two sets of values is small, but one could hypothesize a critical point between them. The structures of the M_2(O-bicyc*)$_6$ compounds refute this: the angles for the proximal ligands lie between 107 and 111°, although the angles for the distal ligands are about 100°. While it is possible that the microcrystalline material on which we performed the Raman experiment was comprised of molecules with all distal ligands (and therefore smaller M−M−O angles), we consider this unlikely given that only one example of an all-distal $M_2(OR)_6$ has been reported $\{Mo_2[OC(CH_3)(CF_3)_2]_6\}$.[8,10] Tellingly, no $\nu_{M\equiv M}$ was observed for this compound despite the presence of Mo−Mo−O angles of 98.2°. We have insufficient data to indicate what structural parameter(s) truly determine our ability to observe $\nu_{M\equiv M}$, but clearly the value of the M−M−X angle does not do so by itself.

Raman Studies. The Raman spectra of the M_2X_6 compounds in this study were taken with 632.8 nm excitation, far to the red of the lowest energy electronic transition in these compounds.[29] Thus, the spectra were acquired under nonresonance conditions, so the $\nu_{M\equiv M}$ band intensities were relatively weak, in contrast to the strong ν_{MM} bands observed in the resonance Raman spectra of quadruply bonded M_2X_8 compounds using laser excitation into the $\delta \rightarrow \delta^*$ absorption band.[30]

To assign a Raman band as $\nu_{M\equiv M}$, we compared the Raman spectra of pairs of Mo_2X_6 and W_2X_6 compounds with identical ligand sets. We looked for a single band in the spectrum of the Mo_2X_6 compound with a reasonable frequency for $\nu_{Mo\equiv Mo}$ (~350−370 cm^{-1})[30,31] that shifted to around 280−300 cm^{-1} in the spectrum of the W_2X_6 compound.[32] In the ideal circumstance in which no vibrational modes couple to $\nu_{M\equiv M}$, only the $\nu_{M\equiv M}$ band should shift between the Mo_2X_6 and W_2X_6 analogues, while all other vibrational bands should exhibit the same frequencies for both. The $M_2(CH_2SiMe_3)_6$ pair and the M_2(O-1-adamantyl)$_6$ pair show nearly ideal behavior in this regard, as seen in Figure 2a,b. We also compared spectra for the same metal and similar ligands, in which the $\nu_{M\equiv M}$ frequency should stay very nearly constant and the ligand frequencies should change. This situation is illustrated in Figure 3 for $Mo_2(CH_2Ph)_6$ vs $Mo_2(CH_2Ph\text{-}4\text{-}Me)_6$. Despite the similarity of the ligands in the pair, they exhibit generally dissimilar spectra, save for the bands at ca. 355 cm^{-1}.[33] This we assign to $\nu_{Mo\equiv Mo}$, an assignment consistent with that derived from comparison of the spectra of $Mo_2(CH_2C_6H_5)_6$ and $W_2(CH_2C_6H_5)_6$.

The Raman frequency data for the 12 pairs of compounds

(24) Becke, A. D. *J. Chem. Phys.* **1993**, *98*, 5648−5652.
(25) Hay, P. J.; Wadt, W. R. *J. Chem. Phys.* **1985**, *82*, 270−283. (b) Wadt, W. R.; Hay, P. J. *J. Chem. Phys.* **1985**, *82*, 284−298. (c) Hay, P. J.; Wadt, W. R. *J. Chem. Phys.* **1985**, *82*, 299−310.
(26) Hay, P. J. Personal communication to T.M.G.
(27) Martin, J. M. L.; Sundermann, A. *J. Chem. Phys.* **2001**, *114*, 3408−3420.
(28) Ehlers, A. W.; Böhme, M.; Dapprich, S.; Gobbi, A.; Höllwarth, A.; Jonas, V.; Köhler, K. F.; Stegmann, R.; Veldkamp, A.; Frenking, G. *Chem. Phys. Lett.* **1993**, *208*, 111−114.
(29) Chisholm, M. H.; Clark, D. L.; Kober, E. M.; van der Sluys, W. G. *Polyhedron* **1987**, *6*, 723−727. (b) Lichtenberger, D. L.; Pollard, J. R.; Gilbert, T. M. Presented at the 205th National Meeting of the American Chemical Society, Denver, CO, Mar/Apr 1993; paper INOR 378.
(30) Cotton, F. A.; Walton, R. A. *Multiple Bonds Between Metal Atoms*, 2nd ed.; Clarendon Press: Oxford, U.K., 1993.
(31) Hopkins, M. D.; Miskowski, V. M.; Gray, H. B. *J. Am. Chem. Soc.* **1986**, *108*, 959−963.
(32) The latter frequency is based on simple mass considerations ($\nu_{Mo\equiv Mo}/\nu_{W\equiv W}$ = 1.38 for the hypothetical bare metal diatomics Mo_2 and W_2 with equal force constants).
(33) The band assigned to $\nu_{Mo\equiv Mo}$ for $Mo_2(CH_2C_6H_4\text{-}4\text{-}Me)_6$ appears at 357 cm^{-1}. We have been unable to prepare the ditungsten analogue of this complex; thus, the pair are not in Table 3.

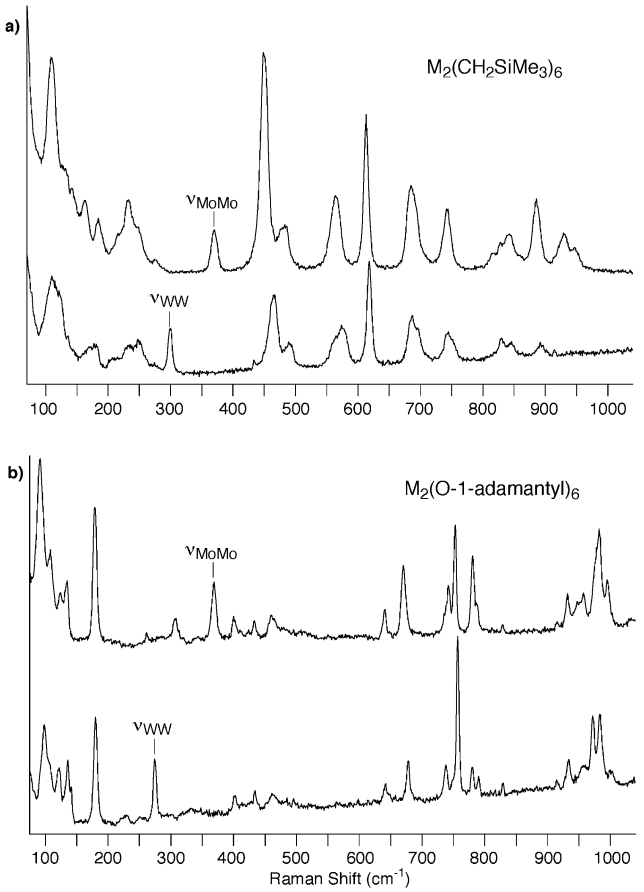

Figure 2. (a) Overlayed Raman spectra of $M_2(CH_2SiMe_3)_6$ (M = Mo, W), showing the similarity of the bands save for those assigned to $\nu_{M\equiv M}$. (b) Overlayed Raman spectra of M_2(O-1-adamantyl)$_6$ (M = Mo, W), showing the similarity of the bands save for those assigned to $\nu_{M\equiv M}$.

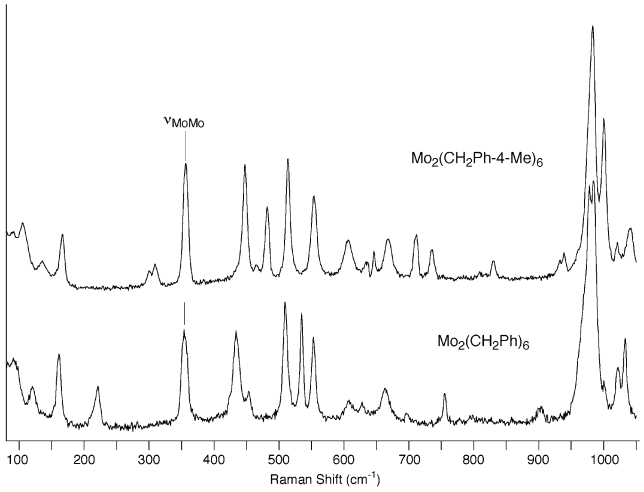

Figure 3. Comparison of the Raman spectra of $Mo_2(CH_2Ph)_6$ and $Mo_2(CH_2Ph\text{-}4\text{-}Me)_6$, showing how most of the bands shift save that assigned to $\nu_{Mo\equiv Mo}$.

(8 hexaalkoxides and 4 hexaalkyls) for which we have identified $\nu_{M\equiv M}$ appear in Table 3. The average metal−metal stretching frequencies (±95% confidence interval) are 366 ± 6 cm^{-1} for the Mo_2X_6 compounds and 287 ± 5 cm^{-1} for the W_2X_6 compounds, with an experimental frequency ratio $\nu_{Mo\equiv Mo}/\nu_{W\equiv W}$ = 1.28 ± 0.02.

The small relative standard deviation of the $\nu_{Mo\equiv Mo}$ and $\nu_{W\equiv W}$ frequencies for a range of ligand sets gives us confidence in the metal−metal stretching assignments. Our assignments also agree with an empirical bond distance/force constant correlation for fifth-row diatomic or pseudodiatomic vibrators.[34] For example, using this correlation and the crystallographically determined Mo≡Mo bond distance of 2.167 Å in $Mo_2(CH_2SiMe_3)_6$,[35] we calculate a force constant of 3.72 mdyne/Å, which in turn yields a predicted frequency of 363 cm^{-1} for the Mo≡Mo diatomic vibrator. This frequency compares well to the observed frequency of 369 cm^{-1} for the Raman band in $Mo_2(CH_2SiMe_3)_6$ that we have assigned as $\nu_{Mo\equiv Mo}$, although our metal−metal stretching force constant of 3.72 mdyne/Å is significantly greater than the average value of 3.37 mdyne/Å derived from molecular mechanics calculations.[36] The empirical bond distance/force constant correlation for sixth-row diatomics[37] predicts a force constant of 3.93 mdyne/Å and $\nu_{W\equiv W}$ = 270 cm^{-1} for $W_2(CH_2SiMe_3)_6$, based on the crystallographic bond distance of 2.254 Å.[17] This compares favorably with the observed frequency of 299 cm^{-1} for the band we have assigned as $\nu_{W\equiv W}$.

Computational Studies. To support our assignments of the metal−metal stretching vibration, we undertook density functional theory calculations. Examples for the classes of M_2X_6 species were optimized, and the optimized structures were used to examine the vibrational modes. The results appear in Table 4. One sees that the unaugmented B3LYP/LANL2DZ and B3LYP/LANL2DZunc;6-31G(d) models give reasonably good agreement with experimental data, but in general the predicted bond lengths are too long. Use of the uncontracted valence basis set does not improve the results much. Addition of a polarization function to the metal (LANL2DZunc+f basis set) improves the predicted metal−metal bond length substantially, reducing the errors to less than 0.01 Å. Using either the LANL2DZ and the 6-31G(d) basis set on the light atoms tends to give M−X bonds that are too long, but the latter gives good agreement for the X−C bonds. Altogether, the B3LYP/LANL2DZunc+f;6-31G(d) model predicts the experimental structures well across the three classes of ligands.

The frequency calculations support the assignments of the experimental data in a remarkably unambiguous fashion. In nearly every case the calculations find a single, distinct vibration which involves a sizable stretch of the metal−metal bond. Typically its frequency differs by ≥50 cm^{-1} from those

(34) Miskowski, V. M.; Dallinger, R. F.; Christoph, G. G.; Morris, D. E.; Spies, G. H.; Woodruff, W. H. *Inorg. Chem.* **1987**, *26*, 2127−2132. $r = 1.83 + 1.51\exp(-F/2.48)$, where r is the internuclear distance in Å and F is the diatomic force constant in mdyne/Å.

(35) Huq, F.; Mowat, W.; Shortland, A.; Skapski, A. C.; Wilkinson, G. *J. Chem. Soc., Chem. Commun.* **1971**, 1079.

(36) Boeyens, J. C. A.; O'Neill, F. M. M. *Inorg. Chem.* **1998**, *37*, 5346−5351. We note that in this work the authors suggest that a value of 3.65 mdyne/Å would be more consistent with the well-determined experimental data for $[Mo_2(HPO_4)_4]^{2-}$. This value is much closer to ours.

(37) Conradson, S. D.; Sattelberger, A. P.; Woodruff, W. H. *J. Am. Chem. Soc.* **1988**, *110*, 1309−1311. $r = 2.01 + 1.31\exp(-F/2.36)$, where r is the internuclear distance in Å and F is the diatomic force constant in mdyne/Å.

nearest, implying little coupling between the mode and ligand-based modes. Interestingly, this applies to the hexaamide complexes, even though experimentally the metal−metal and ligand-based modes are thought to couple. We will return to this point later. The lack of large motions of ligand atoms within the calculated mode further supports the assignment as ν_{MM}.

Both experimentally and theoretically, $\nu_{M\equiv M}$ values for the hexaalkoxides and hexaalkyls are nearly identical, despite the substantial difference in the metal−metal and metal−ligand bond distances. In contrast, the model predicts that the hexaamides will exhibit $\nu_{M\equiv M}$ bands at significantly higher frequencies. This result does not correlate with the M≡M or M−X bond lengths, which as expected fall between those for the hexaalkyls and hexaalkoxides. It may reflect enhanced coupling of $\nu_{M\equiv M}$ with a higher energy ligand-based mode present exclusively in the hexaamides, in keeping with Cotton and Chisholm's inability to observe $\nu_{M\equiv M}$ in these dimers.

Although the agreement between the experimental and theoretical structures improved when polarization functions were added to the basis set, the predicted values of $\nu_{M\equiv M}$ proved insensitive to the improvement (Table 4). We conclude that if one is interested solely in predicting values of $\nu_{M\equiv M}$, then the computationally fast B3LYP/LANL2DZ model can be used to estimate them with minimal loss of accuracy. The more computationally intensive B3LYP/LANL2DZunc+f;6-31G(d) approach is required only for predicting geometries accurately. In this regard, we note work from Cotton and Feng[38] that showed that the predicted ν_{MM} for a series of quadruply bonded metal−metal compounds is fairly insensitive to the size of the basis set employed.

Comparison of the predicted frequencies with the experimental data shows that the calculations consistently overestimate the vibrational energy by an average of 7%. This suggests a scaling factor of ca. 0.93. This is in the correct direction when compared with the scaling factor of 0.8695 derived by Cundari and Raby for the TM═Ch stretching modes in a series of transition metal−chalcogenide compounds, using the RHF/SBKd approach.[39] One expects better accuracy (and thus a scaling factor closer to 1.0) for a correlation-containing model such as B3LYP.[40,41] Applying the scaling factor lowers the absolute disagreement between experimental and predicted $\nu_{M\equiv M}$ values to ca. 2%.

We calculated the scaling factor even though the data set contains only four comparisons to examine why Cotton and Chisholm could not identify $\nu_{M\equiv M}$ in the hexaamide complexes despite our finding computationally that this mode should not be more coupled with ligand-cased modes than in the hexaalkyl and hexaalkoxide cases. The computational data and commentary in their papers suggest they may not have looked in the correct spectral region. Using a general relation between the metal−metal bond length and force constant, they suggested that $\nu_{Mo\equiv Mo}$ should lie near 333 cm^{-1}. A reasonably isolated and intense band at 319 cm^{-1} was observed in the Raman spectrum of $Mo_2[N(CH_3)_2]_6$, but this band also appeared in the spectrum of the tungsten analogue. Furthermore, it shifted dramatically in the spectra of the deuterated analogues, indicating that it does not correspond to a metal-only vibrational mode.

The computational data suggest scaled values of 407 and 347 cm^{-1} for $\nu_{Mo\equiv Mo}$ and $\nu_{W\equiv W}$, respectively. These lie well above the region expected by Cotton and Chisholm. The published spectra are difficult to read clearly, but a rather weak band appears at ca. 415 cm^{-1} in the Raman spectrum of $Mo_2[N(CH_3)_2]_6$; this band shifts only to about 405 cm^{-1} in the deuterated compound.[6] Its size and position make it understandable that it may have been overlooked. A corresponding band appears at ca. 350 cm^{-1} in the Raman spectrum of $W_2[N(CH_3)_2]_6$.[7] It is more intense than expected when compared to the analogous band for the Mo analogue; however, this is consistent with the computational data, which predict greater intensity for the W≡W band. We therefore suggest that the $\nu_{M\equiv M}$ bands are indeed observable in the experimental spectra of the hexaamides but were overlooked owing to their intensities and unexpected energies.

Conclusions

We have confirmed that a variety of M_2X_6 compounds give Raman spectra that allow identification of a band corresponding to $\nu_{M\equiv M}$. The general requirement for making such a compound is that X must be sterically bulky, but precisely why this is necessary remains elusive. The structural data demonstrate that complexes with M−M−O angles substantially greater than 90° can still avoid mode coupling sufficiently to allow observation of $\nu_{M\equiv M}$. Thus, while the vast number of compounds we studied that did not exhibit a band assignable to $\nu_{M\equiv M}$ [some 20, including fairly bulky species such as M_2(O-cyclohexyl)$_6$] serves to indicate that this angle contributes sizably to one's ability to observe it, more subtle structural factors must contribute as well. Unfortunately, the difficulties associated with obtaining disorder-free crystals of these systems limits the structural data available to test possible contributors.

The computational results suggest that this approach may allow more detailed investigation of the issues underlying the identification of $\nu_{M\equiv M}$. That the frequency calculations appear insensitive to augmentation of the LANL2DZ basis set means that such computations for molecules larger than those studied above remain laborious, but they can be accomplished without resorting to augmentation. The assignment of possible $\nu_{M\equiv M}$ bands in the published spectra of $M_2(NMe_2)_6$ at unexpected frequencies points out how computer modeling can attack experimental problems arising from chemical intuition/expectation. We look forward to seeing if new experiments bear out the computational predictions for the hexaamides and plan to examine com-

(38) Cotton, F. A.; Feng, X. *J. Am. Chem. Soc.* **1997**, *119*, 7514−7520. (b) Cotton, F. A.; Feng, X. *J. Am. Chem. Soc.* **1998**, *120*, 3387−3397.
(39) Cundari, T. R.; Raby, P. D. *J. Phys. Chem A* **1997**, *101*, 5783−5788.
(40) This is generally observed with all-electron basis sets: Scott, A. P.; Radom, L. *J. Phys. Chem.* **1996**, *100*, 16502−16513.
(41) Bytheway suggests a scaling factor of 0.9978 for the B3LYP/LANL2DZ approach for a set of singly bonded main group and transition metal complexes. See: Bytheway, I.; Wong, M. W. *Chem. Phys. Lett.* **1998**, *282*, 219−226.

putationally the relationship between structural parameters and the ability to identify $\nu_{M\equiv M}$.

Acknowledgment. T.M.G. acknowledges the donors of the Petroleum Research Fund, administered by the American Chemical Society, and the Northern Illinois University Graduate School Research and Artistry Fund for partial support of this research. R.F.D., J.C.L., M.A.V., and C.E.T. acknowledge support from the Wabash College Haines Research Fund and from the Dow Chemical Co. Foundation. The NIU Computational Chemistry Laboratory (NIU CCL) and the NIU X-ray Diffraction Facility are supported in part by the taxpayers of the State of Illinois; the former also benefited from support by U.S. Department of Education Grant P116Z020095.

Supporting Information Available: Optimized [B3LYP/LANL2DZunc+f;6-31G(d)] Cartesian coordinates for $M_2[OC(CH_3)_3]_6$, $M_2[CH_2C(CH_3)_3]_6$, and $M_2[N(CH_3)_2]_6$ (M = Mo, W) and CIF files for M_2(O-1-4-pentyl[2.2.2]bicyclooctyl)$_6$ (M = Mo, W). This material is available free of charge via the Internet at http://pubs.acs.org.

IC030246F